

A steady and quasi-steady state analysis on the CO₂ hybrid ground-coupled heat pumping system

Zhequan Jin ^(a), Trygve M. Eikevik ^(a), Petter Nekså ^(b), Armin Hafner ^(a)

^(a) Norwegian University of Science and Technology, Kolbjorn Hejes vei 1B, Trondheim, NO-7491, Norway

^(b) SINTEF Energy Research, Kolbjorn Hejes vei 1D, Trondheim, NO-7465, Norway

^(*) Corresponding author. Tel: +47 73593197; fax: +47 73593580; E-mail: zhequan.jin@ntnu.no

Highlights

- A steady state analysis of a CO₂ hybrid transcritical cycle was performed.
- An optimal control strategy of the gas cooler pressure was proposed for a CO₂ hybrid transcritical cycle.
- A ground thermal imbalance performance was defined, and its relation with Φ_{air} was introduced.
- A quasi-steady state model of the CO₂ hybrid ground-coupled heat pumping system was constructed.
- The practical energy efficiency of the CO₂ hybrid ground-coupled heat pumping system was predicted.

Abstract This article contains the steady and quasi-steady state analysis on a CO₂ hybrid ground-coupled heat pumping system for warm climates. The hybrid system uses a combination of ambient air and ground boreholes as a heat sink for the cooling mode, while only the ground boreholes are used as a heat source in the heating mode. The steady state analysis suggests that the optimal control strategy of gas cooler pressure for a CO₂ hybrid transcritical cycle is based on the optimal cooling COP value and the ratio of heat rejected to ambient air. This optimal control strategy is important for decreasing the annual ground thermal imbalance performance of ground boreholes. In addition, the quasi-steady state model of a CO₂ hybrid ground-coupled heat pumping system is constructed for the hourly simulation with different boundary conditions. Simulation results show the details of the system operating characteristics both for heating and cooling mode and the COP values with different operating and design conditions are presented.

Keyword CO₂; Transcritical cycle; Hybrid ground-coupled heat pump; Optimal control strategy

Nomenclature

D	Diameter (mm)
P	Pressure (bar)
Q	Heat (kJ)
\dot{Q}	Heat capacity (W)
T	Temperature (°C)
W	Work (kJ)
\dot{W}	Power (W)

Greek symbols

Δh	Enthalpy difference (J kg^{-1})
α	Heat transfer coefficient ($\text{W}\cdot\text{m}^{-2}\cdot\text{K}^{-1}$)
π	Compressor pressure ratio
φ	Instantaneous ratio of heat rejected to ambient air to the evaporating heat
Φ	Yearly averaged ratio of heat rejected to ambient air to the evaporating heat

Subscripts

air	Ambient air
c	Cooling mode
comp	Compressor
evp	Evaporator
gc	Gas cooling
h	Heating mode
hp	Heat pump
hp,c	Heat pump unit, cooling
hp,h	Heat pump unit, heating
i	In
o	Out
min	Minimal
max	Maximal
r	Return
s	Supply
space	Building indoor space
total,c	Heat pump system, cooling mode
total,h	Heat pump system, heating mode
w	Water

Abbreviation

AHX	Air side heat exchanger
ASHP	Air source heat pumping
COP	Coefficient of performance
CO ₂	Carbon dioxide
GCHP	Ground-coupled heat pumping
GHX	Ground heat exchanger
GTIP	Ground thermal imbalance performance
H ₂ O	Water
HX	Heat exchanger
IPLV	Integrated Part Load Value
sCOP	Seasonal COP

1. Introduction

From the point of view of environmental sustainability and energy conservation, the combination of sustainable energy technology with environment friendly refrigerants can be an important trend for the future development of the refrigeration, air conditioning and heat pump industry. As a type of natural refrigerant, CO₂ (R744) shows great potential as the dominant refrigerant in the future due to its environmental characteristics and superior thermodynamic properties.

1 As is well known, Lorentzen (1990) first proposed the modern use of CO₂ in a transcritical cycle, and this
2 was a turning point for the revival of CO₂ as a refrigerant. So far, the CO₂ refrigerant, based on the
3 transcritical cycle, has been quickly and successfully commercialized in the supermarket refrigeration and
4 heat pump industry. For example, more than 4000 CO₂ transcritical refrigeration systems were installed
5 throughout the European countries by 2015, and this number has increased from 1300 in 2011 (Masson,
6 2015). In addition, a new concept of CO₂ application in Norwegian supermarkets, which covers cooling,
7 heating, ventilation and air conditioning, was successfully created by SINTEF Energy Research centre
8 (Hafner et al., 2014). The application of CO₂ in the air conditioning industry is still in the research stage, and
9 there are only a few reports or literature references about the application of CO₂ in the air conditioning
10 industry (Jakobsen et al., 2004, 2007; Neksa et al., 2010). This indicates the need to search for possible
11 enhancements to reach sufficiently high efficiency at the highest ambient temperatures. In addition, it is
12 worth noting that most of the applications of the CO₂ refrigerant for transcritical storage are limited to the
13 relatively cold regions, due to the energy efficiency of the system. However, some research work has tried to
14 expand the use of this natural refrigerant to warmer climates by introducing the latest technology to decrease
15 the work losses in the transcritical cycle. For example, the CO₂ transcritical ejector system shows good
16 energy performance under warm climate conditions, where the average ambient temperature is higher than
17 that of a cold climate. Moreover, the combination of the heat sinks with different temperature levels, like
18 ambient air and ground soil, is also a good solution to expand the use of the CO₂ refrigerant to the warmer
19 climates. The combination of an air-cooled CO₂ system with ground boreholes might be a means to increase
20 the efficiency, and, to the authors' knowledge, there are few references available. Regarding the GCHP
21 system, Esen et al. (2007) techno-economically compared the ground-coupled and air-cooled heat pumping
22 system for the indoor cooling mode, and it was observed that performance of the GCHP system is much
23 better. However, the underground heat accumulation in a warm climate area will increase the ground
24 temperature, which can consequently deteriorate the performance of a GCHP system over time. Further
25 efforts were made to investigate the hybrid GCHP system, which employs a supplemental heat rejecter or
26 heat absorber with the GCHP system (Kavanaugh, 1998; Man et al., 2010; Esen et al. 2015).

27 Since there is a big temperature glide in the heat rejection process, as well as in the high ambient temperature
28 operation, some of the heat can still be released to the ambient air due to a high operation temperature in the
29 gas cooler of the CO₂ transcritical heat pump cycle. Better performance of the CO₂ heat pumping system,
30 and elimination of the underground heat accumulation, could be the benefits from introducing reasonable
31 supplemental heat rejecters to the GCHP. So in this work, the steady state and quasi-steady state analysis on
32 a CO₂ hybrid ground-coupled heat pumping system is performed for a warm climate. The main objectives
33 are determination of the optimal control strategy of the gas cooler pressure, and prediction of the practical
34 energy efficiency of the CO₂ hybrid ground-coupled heat pumping system.

2. CO₂ hybrid ground-coupled heat pumping system description

The developed CO₂ hybrid ground-coupled heat pumping system aims to cover the indoor heating and cooling load for buildings as a central plant. The CO₂ heat pumping system is mainly composed by a CO₂ refrigerant loop and three heat transfer fluid loops, which include an indoor fan coil loop, a ground borehole loop, and an open ambient air cooling loop, as shown in Figure 1.

The CO₂ heat pump unit in the refrigerant loop, which is based on a classical reverse transcritical cycle, features two separate gas coolers in a heat rejection process. So the advantage of a large temperature glide under the same isobars could be used to reject the gas cooling heat to different temperature levels. Moreover, during the indoor cooling mode, the temperature glide of CO₂ offers the possibility to reject part of the heat with a high temperature to ambient air through the open ambient air cooling loop. For example, the transcritical CO₂ fluid from the outlet of the compressor can first reject heat to the air-cooled gas cooler; afterwards the circulating water (heat transfer fluid) from the ground boreholes will be used to cool down the CO₂ in the water-cooled gas cooler to improve the system's performance. The ground borehole loop and fan coil loop form the other heat transfer fluid loops. Ground boreholes can work as heat sinks, combining with ambient air in the indoor cooling mode (open solid line valve and closed dotted line valve in Figure 1), or as the only heat source in the indoor heating mode (open dotted line valve and closed solid line valve). On the other hand, the fan coil could satisfy the indoor heating and cooling load of the buildings. It should be mentioned that the open ambient air cooling loop only operates during the indoor cooling mode.

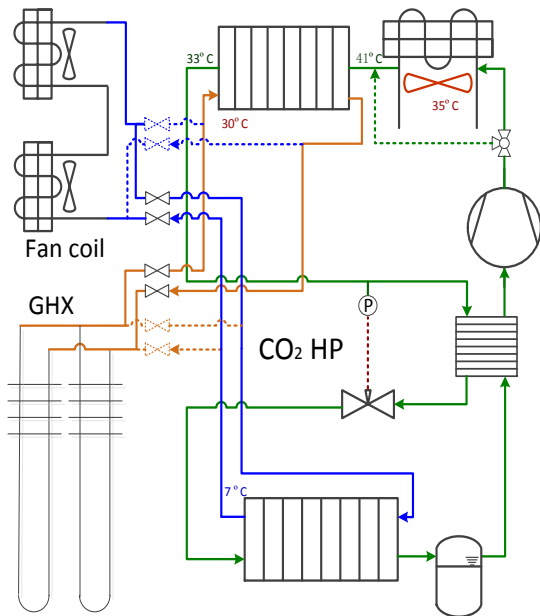


Fig. 1 - Schematic diagram of the CO₂ hybrid ground-coupled heat pumping system

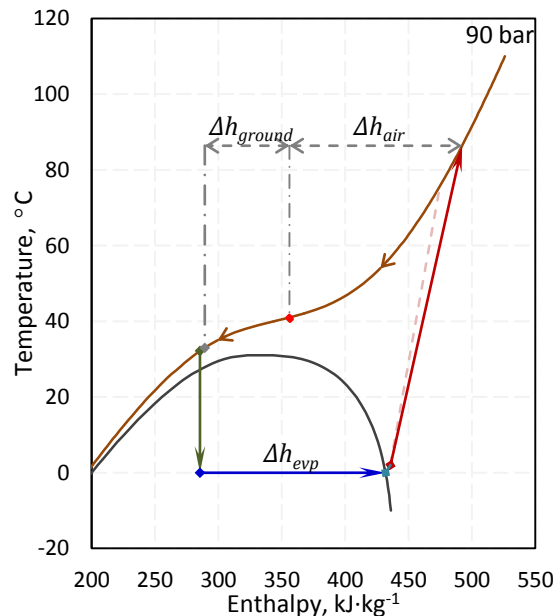


Fig. 2 - Hybrid cooling CO₂ transcritical cycle in a T-h diagram

Figure 2 shows the hybrid cooling CO₂ transcritical cycle in a T-h diagram. The cycle and diagram are drawn to indicate the full load operating conditions, and show the intermediate state between the two gas coolers. As shown in the figure, this intermediate state between the two gas coolers is given by 41 °C and 356 kJ·kg⁻¹.

So, it is clear that the gas cooling heat, expressed as the difference in enthalpy in the diagram, is divided into two parts by the separate air and water-cooled gas coolers. The share of Δh_{air} and Δh_{ground} can be regulated by the gas cooling pressure, while the CO_2 temperature at the separation point is determined by the ambient air condition. This characteristic of the hybrid cooling CO_2 transcritical cycle offers the optimal regulation strategy of a gas cooler pressure, which will be discussed in the following section.

3. The steady state analysis of a hybrid CO_2 transcritical cycle

In order to better understand this cycle characteristic, a steady analysis of the hybrid CO_2 transcritical cycle is performed for different operating conditions. The selected operating conditions are inspired from the idea of Integrated Part Load Value (IPLV). A performance characteristic, IPLV is most commonly used to describe the performance of a plant capable of capacity modulation. The IPLV is calculated using the efficiency of the equipment while operating at capacities of 100%, 75%, 50%, and 25% (AHRI, 2011). As mentioned in the introduction, the hybrid CO_2 GCHP system will be applied under the warm climate conditions, with the aim to improve the energy efficiency and balance the ground boreholes' heat exchange. Steady state analysis only investigates the cooling performance of the hybrid CO_2 GCHP system, which aims to provide the fundamental information for the hybrid CO_2 GCHP system design procedure.

Theoretically, the efficiencies of a chiller or heat pump under different operating capacities can be calculated with corresponding standard rating conditions. However, it is necessary to specify both evaporating and condensing (gas cooling for transcritical cycle) side conditions, which mainly include the inlet temperature and flow rate requirement of the heat transfer fluid. Since the environmental parameters of Shanghai, China will be used in the practical simulation, the rating conditions referred to be the Chinese National Standard GB/T 18430.1-2007. Table 1 shows the heat transfer fluid temperature and flow rate requirement for a hybrid CO_2 transcritical system, meanwhile the temperature difference between the CO_2 and the heat transfer media at the outlet of two gas coolers is also suggested by considering the heat transfer performance of the gas cooling heat exchangers.

Table 1 – Full and partial cooling load rating conditions for the hybrid CO_2 transcritical system

Load value	Ground side gas cooler		Air side gas cooler		Evaporator	Water flow rate, $\text{m}^3 \text{h}^{-1} \text{kW}^{-1}$
	$T_{\text{return water}}, ^\circ\text{C}$	$T_{\text{approach with } \text{CO}_2}, \text{K}$	$T_{\text{ambient air}}, ^\circ\text{C}$	$T_{\text{approach with } \text{CO}_2}, \text{K}$	$T_{\text{supply cooling water}}, ^\circ\text{C}$	
100%	30	3	35	6	7	0.172
75%	26	2	31.5	5		
50%	23	1	28	4		
25%	19	0.5	24.5	3		

Table 2 lists a group of reference parameters for a theoretical analysis of the CO_2 transcritical cycle under different operating conditions according to the practical system. With the following parameters, the enthalpy

based CO₂ transcritical cycles can be easily constructed in a $T-h$ diagram, as shown in Figure 2 in the previous section.

Table 2 – Parameter specifications of the CO₂ transcritical cycle for different operating conditions

Items	100%	75%	50%	25%
Evaporating temperature, °C	0.0	2.0	3.5	4.3
Isentropic efficiency, -	0.71 (Hafner et al., 2013)			
Overheating temperature, K	2.0			
Gas cooler pressure, bar	78 ~ 122			
CO ₂ outlet T from air-cooled gas cooler, °C	41.0	36.5	32.0	27.5
CO ₂ outlet T from water-cooled gas cooler, °C	33.0	28.0	24.0	19.5

One of the main objectives of this theoretical analysis is to find the control strategy for the practical system. Actually, there are two important indexes for the CO₂ hybrid GCHP system. One is the COP_c value, which can indicate the instantaneous energy efficiency of the system, the other is the φ_{air} value, which means the operating ratio of the heat rejected to ambient air and the evaporating heat, as shown in Eq. 1.

$$\varphi_{\text{air}} = \frac{\Delta h_{\text{gc,air}}}{\Delta h_{\text{evp}}} \quad (1)$$

The theoretical calculation results of COP_c and φ_{air} values under different pressures for four operating conditions are shown in Figure 3 and 4.

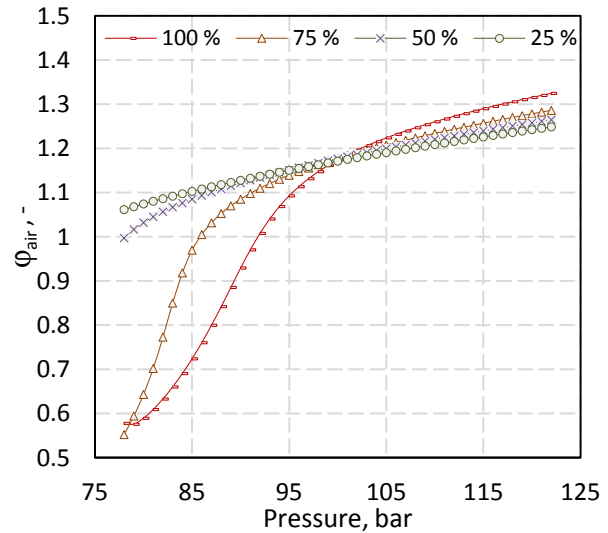
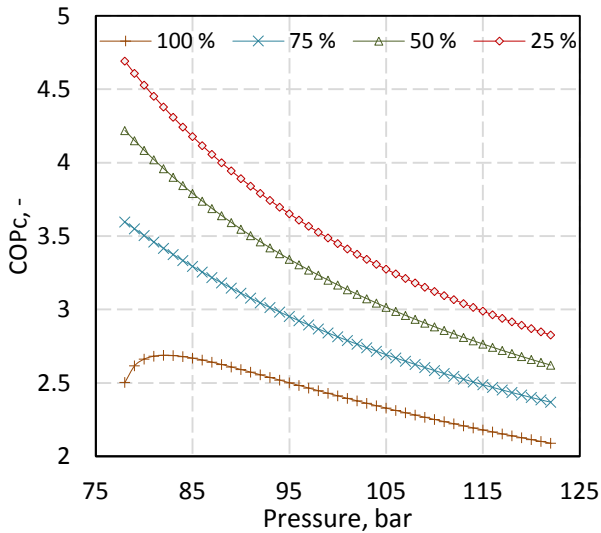


Fig. 3 - COP_c value for different gas cooler pressures

Fig. 4 - φ_{air} value for different gas cooler pressures

As a whole, it can be observed that the theoretical COP_c decreases and the φ_{air} value increases with increased gas cooler pressure for different operating conditions. Therefore, the higher COP_c is conflicting with a higher φ_{air} value for the same hybrid cooling CO₂ transcritical cycle. However, the meaning of the φ_{air} value is of importance for the hybrid ground-coupled heat pumping system, because it directly influences the ground

thermal imbalance performance (GTIP). The GTIP value is generally controlled to be 0% , to maintain the stable energy efficiency of the GCHP system for long terms operation. The calculation method of the GTIP value and its internal relation with the Φ_{air} value, which means the yearly averaged ratio of heat rejected to ambient air and the evaporating heat, are introduced by following Eq. 2 to Eq. 7.

In order to ensure the GTIP value is a positive number, the $GTIP_c$ and $GTIP_h$ are defined separately based on whether the building load is heating dominated or cooling dominated.

$$GTIP_c = \left(1 - \frac{\sum_{cooling} Q_{borehole}}{\sum_{heating} Q_{borehole}} \right) \times 100 \% \quad \text{or} \quad GTIP_h = \left(1 - \frac{\sum_{cooling} Q_{borehole}}{\sum_{heating} Q_{borehole}} \right) \times 100 \% \quad (2)$$

If the amount of heat rejected to the borehole during the cooling mode equals to that absorbed during the heating mode, the value of the GTIP can be 0%. This is an important design criterion for the CO₂ hybrid ground-coupled heat pumping system:

$$\sum_{cooling} Q_{borehole} = \sum_{heating} Q_{borehole}, \text{ when } GTIP_c = 0 \quad (3)$$

It should be mentioned, this design criterion is restricted in a situation that is not considering the influence of the underground water flow or heat exchange on vertical direction (including with the ground surface).

According to the energy conservation equation for the hybrid cooling CO₂ transcritical cycle, Eq. 4 and 5 can be used for the cooling and heating mode:

$$\sum_{cooling} Q_{borehole} + \sum_{cooling} Q_{air} = \sum_{cooling} Q_{space} + \sum_{cooling} W_{comp} \quad (4)$$

$$\sum_{heating} Q_{borehole} = \sum_{heating} Q_{space} - \sum_{heating} W_{comp} \quad (5)$$

The seasonal coefficient of performance (sCOP) for the heating and cooling mode is defined as follows:

$$sCOP_c = \frac{\sum_{cooling} Q_{space}}{\sum_{cooling} W_{comp}}; \quad sCOP_h = \frac{\sum_{heating} Q_{space}}{\sum_{heating} W_{comp}} \quad (6)$$

Once the building load characteristic and the sCOP of the heat pumping system are determined, then the Φ_{air} value, one of the most important design criteria of the specified CO₂ hybrid ground-coupled heat pumping system, can be calculated by Eq. 7:

$$\Phi_{\text{air}}|_{\text{GTIP}=0} = \frac{\sum_{\text{cooling}} Q_{\text{air}}}{\sum_{\text{cooling}} Q_{\text{space}}} = \frac{\sum_{\text{cooling}} Q_{\text{space}} \times \left(I + \frac{1}{\text{sCOP}_c} \right) - \sum_{\text{heating}} Q_{\text{space}} \times \left(I - \frac{1}{\text{sCOP}_h} \right)}{\sum_{\text{cooling}} Q_{\text{space}}} \quad (7)$$

On the other hand, it is important to ensure that the annual averaged ϕ_{air} value (instantaneous value) approaches the Φ_{air} value (yearly averaged value), especially for the long term energy efficiency of the hybrid CO₂ system under warm climate conditions. The minimum operating pressure and optimal operating pressure mode is adopted for the control of the hybrid system. The minimum operating pressure refers to the pressure that is determined to achieve the required Φ_{air} value under the operating conditions, which is subsequently used to calculate the IPLV for 75 % of the system capacity, as shown in table 3. This is mainly because 75 % is a moderate value in the IPLV concept, which can make a yearly balance between energy efficiency and the ground thermal imbalance performance of the hybrid ground-coupled heat pumping system. For the optimal gas cooling pressure operating mode, the correlation of optimal pressure can be calculated with the CO₂ gas cooler outlet temperature, evaporating temperature, and isentropic efficiency (Liao et al., 2000).

Table 3 - Specification of the gas cooler pressure for different Φ_{air} value

Φ_{air}	0.8	0.9	1.0	1.1	1.2
Minimum operating pressure, bar	82.4	83.7	85.9	91.2	103.6

The switching signal for the gas cooler pressure regulation can be activated based on the tested value of the gas cooling pressure. When the tested value from the pressure sensor is bigger than the minimum operating pressure, the control signal will switch to the optimal pressure mode. However, the signal for the minimum operating pressure will be activated; when the tested gas cooling pressure is lower than the minimum operating pressure. The main control strategy is shown in Figure 5, which includes the control strategy both for the heating and cooling mode. The gas cooling pressure control strategy of the heating mode is similar to the cooling mode, but the minimum pressure is replaced by the maximum pressure. The maximum pressure will limit the highest pressure of gas cooler for safety reasons, but the control signal will switch to the optimal pressure mode when the tested value of the gas cooling pressure is lower than the maximum operating pressure.

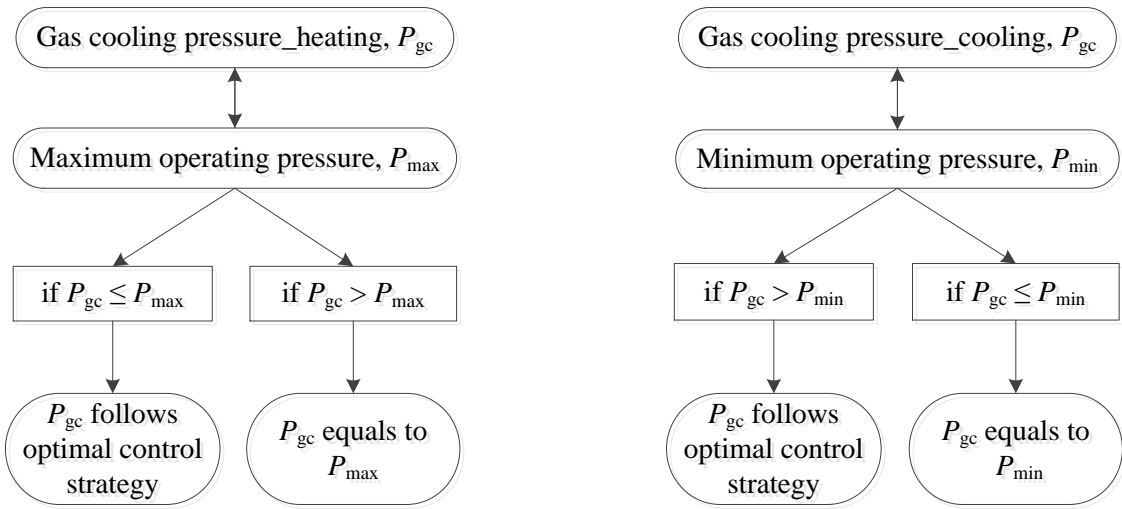


Fig. 5 - Control logics for the optimal gas cooling pressure for the heating and cooling mode

To summarize, the steady state analysis of the CO₂ hybrid GCHP system can well support the fundamental design procedure of the quasi-steady state model for the CO₂ system by setting reasonable boundary conditions.

4. Quasi-steady state simulation of the hybrid CO₂ transcritical cycle

In this section, the quasi-steady state analysis of the hybrid CO₂ transcritical GCHP system is conducted by means of an hourly simulation in the Modelica environment. Compared with the building TRNSYS modelling work (Byrne et al., 2009; Deng et al., 2013), which focuses on the building's thermal energy performance by using the steady state heating and cooling capacities and the COP, this work focuses more on the time independent heat pumping system's performance. In other words, this quasi-steady state analysis aims to predict the energy performance of the practical CO₂ system under different operating conditions. Table 4 summarizes the main difference between the steady state analysis and the quasi-steady state analysis.

Table 4 – The main difference between steady state analysis and quasi-steady state analysis

Analysis mode	Steady state analysis	Quasi-steady state analysis
Compressor isentropic efficiency	Constant with π value	Variable with different π value
Compressor capacity control	No control	Controlled by the cooling load
Expansion valve control	No, isenthalpic process	Yes, optimal pressure control strategy
Heat exchanger performance	Without heat transfer loss	With heat transfer loss
Work of pump and fan	No	Yes
Operating condition	Fixed according to IPLV standard conditions	Varying environmental conditions based on the weather data

As shown in Table 4, the quasi-steady state analysis aims to insure that the hourly operating characteristic of the developed quasi-steady state models is comparable with that of the field heat pumping facility. This can also be observed from the schematic diagrams of the CO₂ hybrid GCHP system configuration.

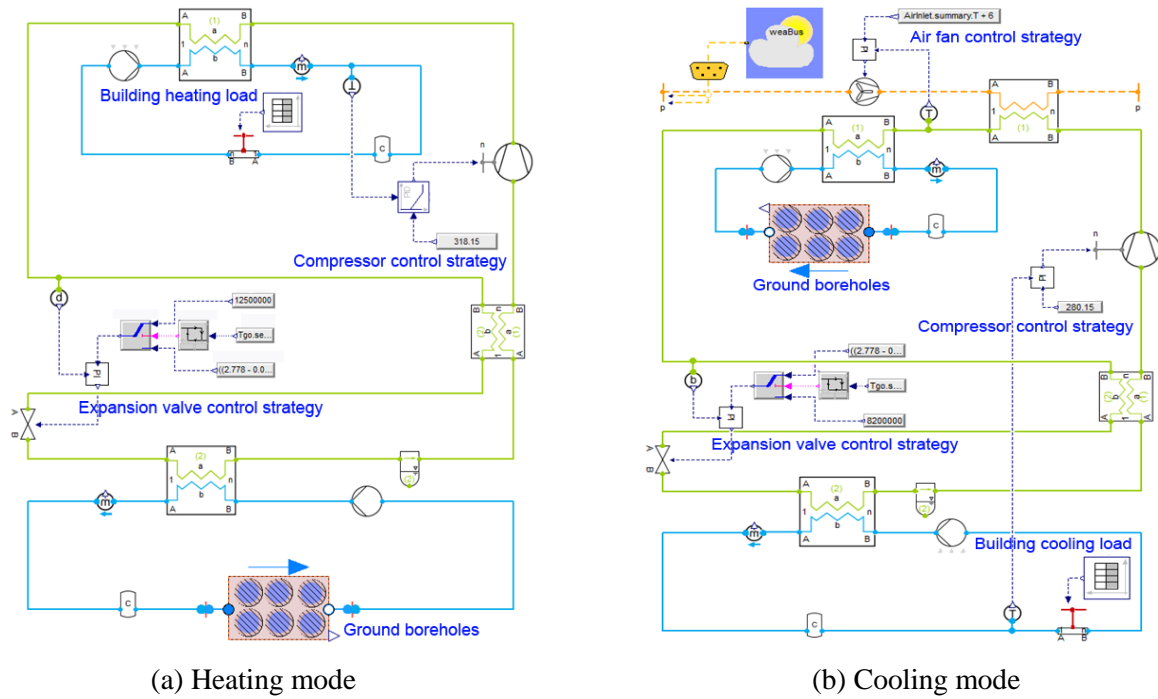


Fig. 6 - Quasi-steady state models of the CO₂ hybrid GCHP system

Figure 6 shows the developed models for the cooling and heating mode based on the concept of the CO₂ hybrid GCHP system. Both of the cooling and heating mode models are integrated with the corresponding control strategies of the different components. For example, the gas cooler pressure control based on the optimal control strategy describe in the previous section, the variable compressor speed control based on the heating/cooling water supply temperature, and the air volume flow control of the air-cooled and ground-cooled gas cooler are all based on the CO₂ outlet temperature from the air-cooled gas cooler. And last, the models of the heat pumping system also integrate the building cooling load and the weather data for the simulation. Figure 7 shows the annual heating and cooling load of the reference building in Shanghai, China. Actually, the peak indoor cooling load value is scaled down to 43 kW, according to the calculation results from Energy Plus (Goel et al., 2014), and the same scale-down principle is applied to the annual indoor air conditioning load profile, as shown in Figure 7.

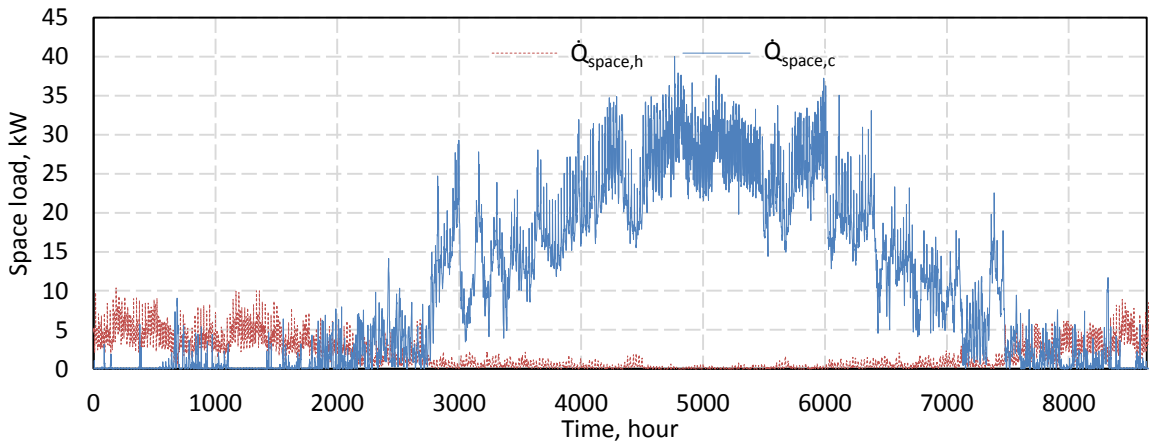


Fig. 7 - Annual heating and cooling load of the reference building in Shanghai, China

In addition, Table 5 summarizes the component specifications and important design parameters of the CO₂ hybrid GCHP system quasi-steady state model. This information is acquired from theoretical calculation or manufacturer's information.

Table 5 - Specifications of the hybrid CO₂ ground-coupled heat pumping system

Components	Type and specification
Compressor	Bock_hgx46_210_4s with variable frequency control
Air-cooled gas cooler	Fin and tube heat exchanger ✓ CO ₂ side: $\alpha_{CO_2}=2500 \text{ W}\cdot\text{m}^{-2}\cdot\text{K}^{-1}$ ✓ Heat transfer model of Haaf, $\text{W}\cdot\text{m}^{-2}\cdot\text{K}^{-1}$ (Haaf, 1988 and Richter, 2008)
Water-cooled gas cooler	Plate heat exchanger (Thome and Ribatski, 2005) ✓ CO ₂ side: $\alpha_{CO_2}=2500 \text{ W}\cdot\text{m}^{-2}\cdot\text{K}^{-1}$ ✓ Water side: $\alpha_w=2500 \text{ W}\cdot\text{m}^{-2}\cdot\text{K}^{-1}$
Water-cooled evaporator	Plate heat exchanger
Expansion device	Back pressure control valve with optimal control strategy
Borehole parameters	Vertical U-tube borehole heat exchanger (Yu et al., 2011)
Environmental condition	Weather and underground condition in Shanghai, China
Load condition	Reference hotel building based on ASHRAE90.1
Parameter items	Values
Cooling capacity, kW	43
Φ_{air} , -	0.8~1.2
Heat flux of borehole, $\text{W}\cdot\text{m}^{-1}$	35 ¹

Note: 1. Heat flux refers to the heat transfer rate (W) of per meter of the borehole length.

Table 6 lists the detail information of the different heat exchangers used for heat pumping systems, which are also from the theoretical calculation and manufacturer information. It should be mentioned, the heat transfer coefficients of CO₂ and H₂O are chosen as averaged values from the literature (Park and Hrnjak., 2007, Thome and Ribatski., 2005).

Table 6 - Simulation boundary conditions for different heat exchangers

Parameters	CO ₂ -hybrid GCHP	CO ₂ -ASHP
$\alpha_{CO_2}, \alpha_{R410A}, \alpha_{H_2O}$ in plate HX	$\alpha_{CO_2}=2500 \text{ W/m}^2\text{K}$ $\alpha_{H_2O}=2500 \text{ W/m}^2\text{K}$	$\alpha_{CO_2}=2500 \text{ W/m}^2\text{K}$ $\alpha_{H_2O}=2500 \text{ W/m}^2\text{K}$
Evaporator (43kW)	Kaori_C095*72 (43.9kW)	Kaori_C095*72 (43.9kW)
Gas cooler - GHX	Kaori_C097*48 (26.37kW)	N/A
Borehole length (q=35W/m)	585m (65m*9)	N/A
$\alpha_{CO_2}, \alpha_{R410A}, \alpha_{\text{air}}$ in AHX	$\alpha_{CO_2}=2500 \text{ W/m}^2\text{K}$ α_{air} by Haaf model	$\alpha_{CO_2}=2500 \text{ W/m}^2\text{K}$ α_{air} by Haaf model
Gas cooler/ Condenser-AHX (Tube $D_i=7\text{mm}$)	length=1.2*5*20 m = 120 m	length=2.2*6*20 m = 264 m

4.1 Simulation results for the indoor cooling mode

The energy performance of the different operating modes is expressed by the coefficient of performance (COP) of the heat pumping system. In this section, the COP_c values of the CO₂ heat pumping unit and system

are used to evaluate the energy performance of the cooling mode, and the calculation equation is shown in Eq. 8 and 9.

$$\text{COP}_{\text{hp,c}} = \frac{\dot{Q}_c}{\dot{W}_{\text{comp}}} \quad (8)$$

$$\text{COP}_{\text{total,c}} = \frac{\dot{Q}_c}{\dot{W}_{\text{comp}} + \dot{W}_{\text{fan}} + \dot{W}_{\text{pump}}} \quad (9)$$

Figure 8 shows the time-dependent COP_c and ϕ_{air} value under different indoor cooling loads during 48 and 24 hours summer periods. The value of the $\text{COP}_{\text{total,c}}$ varies from 2.2 to 4.1, and the $\text{COP}_{\text{hp,c}}$ changes from 2.3 to 4.2 when the cooling load varies from 30 % to 95 %. It is obvious that the $\text{COP}_{\text{total,c}}$ is always lower than the $\text{COP}_{\text{hp,c}}$ due to the additional airside fan and hydraulic pump work. However, the difference is getting smaller with each increment of the compressor's effect, because the compressor takes the major share of the total energy consumption in high cooling load conditions. In addition, these results are based on a quasi-steady state model when the design ϕ_{air} value is 1.1, so the operating ϕ_{air} value varies around 1.1 under different cooling load conditions.

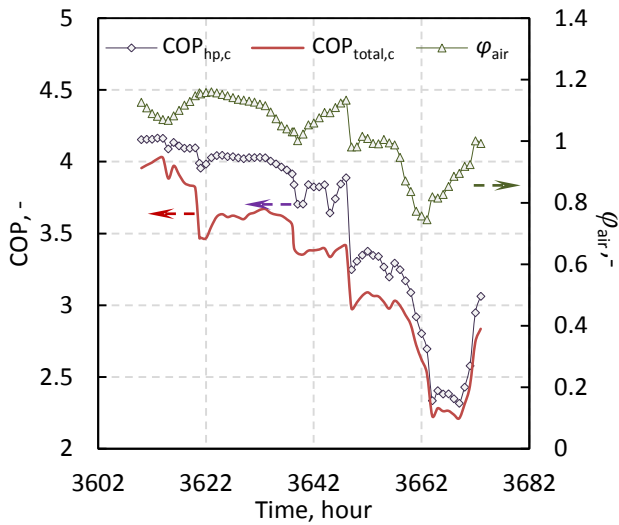


Fig. 8 - COP_c and ϕ_{air} values under different indoor cooling loads

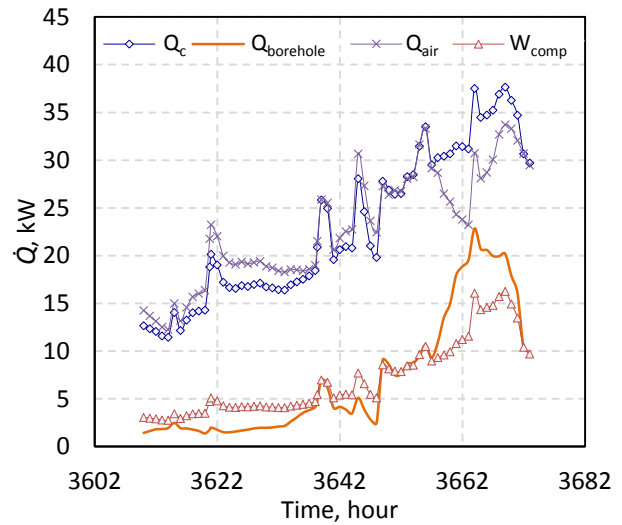


Fig. 9 - Heat transfer amount of different CO_2 system components for the indoor cooling mode

The heat transfer rate and power consumption of the different components are shown in Figure 9. The \dot{Q}_c refers to the cooling capacity of the heat pumping system, and the values are the same as the cooling load of the reference building. The power consumption of the compressor is mainly depending on the cooling load of the system. This is the reason that the variation tendency of the compressor work and cooling capacity is very similar. In addition, Figure 9 also shows that the CO_2 hybrid GCHP rejects more of the heat to the ambient air than to the ground borehole, especially when the cooling load or ambient temperature is low. However, the heat rejection rate to the ground borehole will be increased when the cooling load and ambient

temperature is increasing. This can be explained by the internal operating pressure and temperature variation in the different components, as shown in Figure 10 and 11. In Figure 10, the optimal control strategy for the hybrid system is activated by the high ambient temperature and cooling load, which caused the variation of the gas cooling pressure. Thus, the different working fluid temperature has an obvious variation when the gas cooling pressure is disturbed, as is shown in Figure 11.

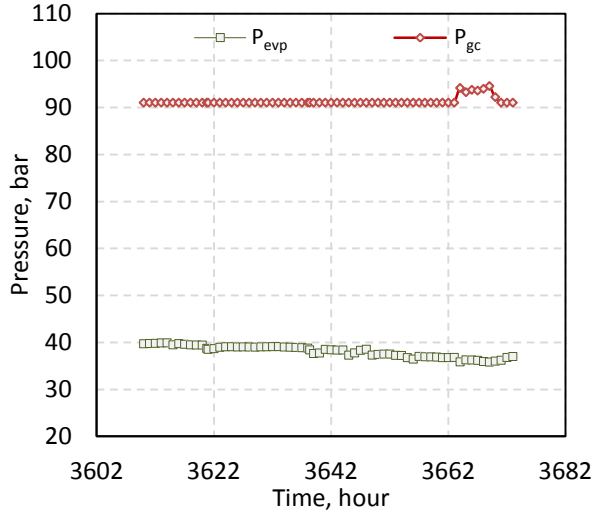


Fig. 10 - Gas cooling and evaporating pressure under different indoor cooling loads

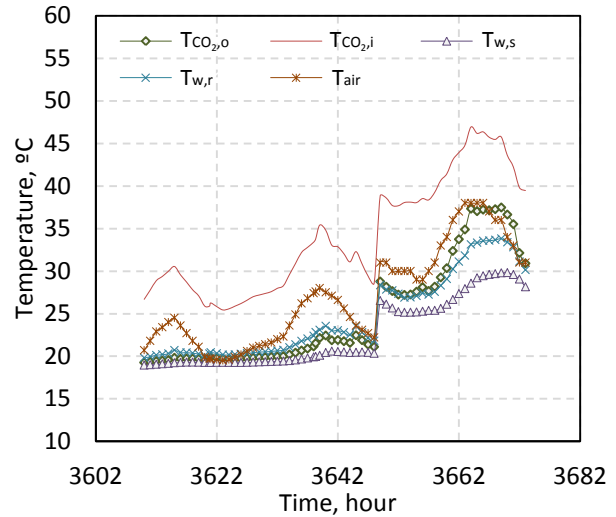


Fig. 11 - Working fluid temperature variation under different indoor cooling loads

As is shown in Table 3, five operating conditions are specified for the different Φ_{air} values. Figures 12 and 13 showed the simulation results of the COP_c and ϕ_{air} variation under different indoor cooling loads for various ϕ_{air} values. It can be observed that the lower Φ_{air} value gives the higher COP_c , especially when the cooling load is at a low level, and this is due to the lower operating gas cooling pressure. However, the ϕ_{air} value variation is contrary to COP_c variation tendency. As it is shown in Figure 13, the higher Φ_{air} value gives the higher ϕ_{air} , and the difference is greater when the cooling load is at a high level.

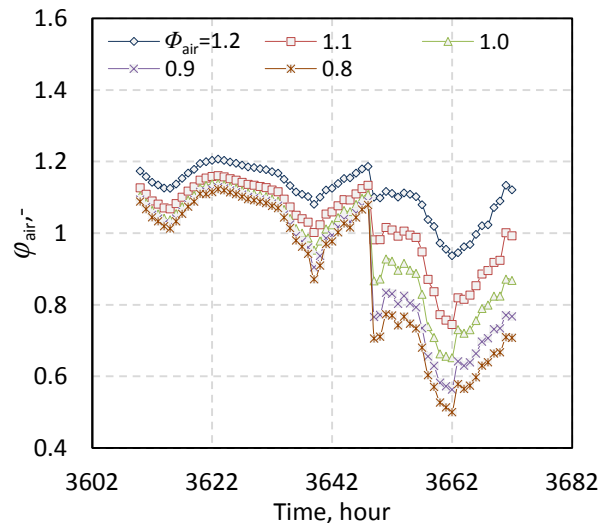
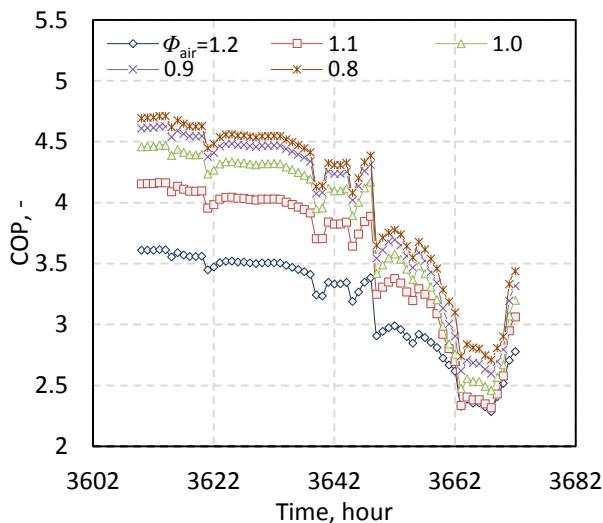


Fig. 12 - COP_c variation under different Φ_{air} values with different indoor cooling loads

Fig.13 - ϕ_{air} variation under different Φ_{air} values with different indoor cooling loads

On the other hand, a CO₂ air source heat pumping (ASHP) system model is also constructed to compare the performance with the CO₂ hybrid GCHP system under different ambient air temperatures for the investigated cooling periods. The developed CO₂ ASHP model only replaced the ground borehole heat exchanger with the corresponding capacity of an air cooled heat exchanger. The CO₂ ASHP system only rejects the gas cooling heat to the ambient air, rather than to the different temperature levels of ambient air and underground boreholes. Figure 14 shows the simulation COP_c results of these two systems under different ambient air temperatures. The ambient air temperature range is 19~38 °C in the selected cooling period of the reference year. It can be observed that the cooling performance of the CO₂ hybrid GCHP system is better than the ASHP system as a whole. The calculated averaged COP_c values are 3.56 and 2.78, respectively, during this period, and the averaged performance improvement is 28.1 %. This improvement is mainly due to the fact that the low temperature of the underground borehole lowers the CO₂ refrigerant outlet temperature from the gas cooler, and then increases the specific refrigeration capacity of the CO₂ hybrid transcritical cycle.

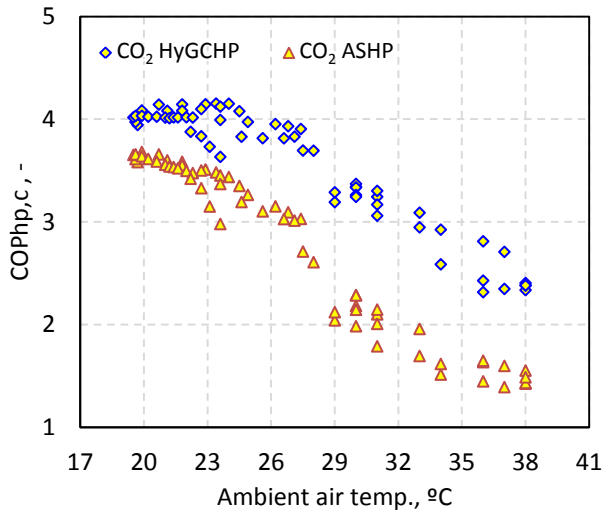


Fig. 14 - COP_c comparison for CO₂ HyGCHP and ASHP at different ambient air temperatures

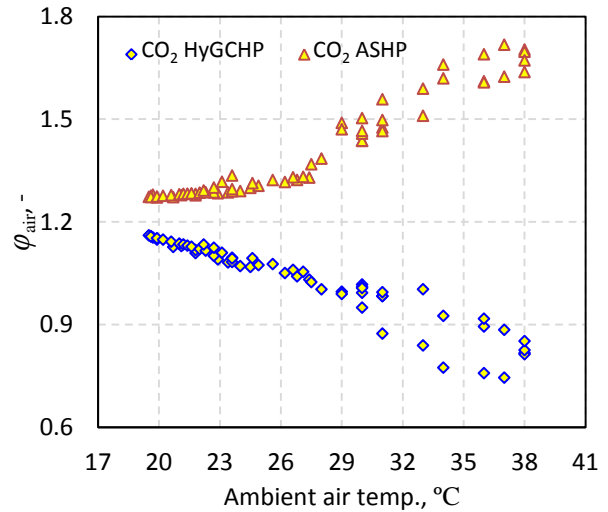


Fig. 15 - ϕ_{air} comparison for CO₂ HyGCHP and ASHP at different ambient air temperatures

Meanwhile, Figure 15 also shows the operating ϕ_{air} value of the two different systems. Since the CO₂ ASHP system only rejects the heat to ambient air, the ϕ_{air} value gradually increases with the higher ambient air temperature. However, the CO₂ hybrid GCHP will reject more gas cooling heat to the ground borehole, and this is the reason that the corresponding ϕ_{air} value decreases with the higher ambient air temperature.

4.2 Simulation results for the indoor heating mode

In this section, the COP_h values of the CO₂ heat pumping unit and system are used to evaluate the energy performance under the heating mode, and Eq. 10 and 11 shows the corresponding calculation equation.

$$\text{COP}_{\text{hp,h}} = \frac{\dot{Q}_h}{\dot{W}_{\text{comp}}} \quad (10)$$

$$\text{COP}_{\text{total,h}} = \frac{\dot{Q}_h}{\dot{W}_{\text{comp}} + \dot{W}_{\text{fan}} + \dot{W}_{\text{pump}}} \quad (11)$$

Figure 16 shows the time-dependent COP_h value under different indoor heating loads during a 72 hour winter period. The value of the $\text{COP}_{\text{total,h}}$ varies from 2.53 to 3.15, and the $\text{COP}_{\text{hp,h}}$ changes from 2.53 to 3.07 when the heating load varies from 30% to 100%. It is observed that the $\text{COP}_{\text{total,h}}$ is always lower than the $\text{COP}_{\text{hp,h}}$ due to the additional hydraulic pump work, but the difference is small compared with the simulation results for the indoor cooling mode. This is because there is no airside fan power consumption for the indoor heating mode.

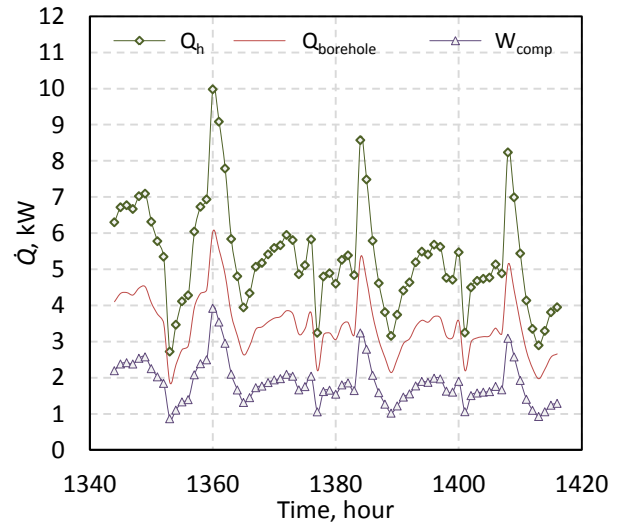
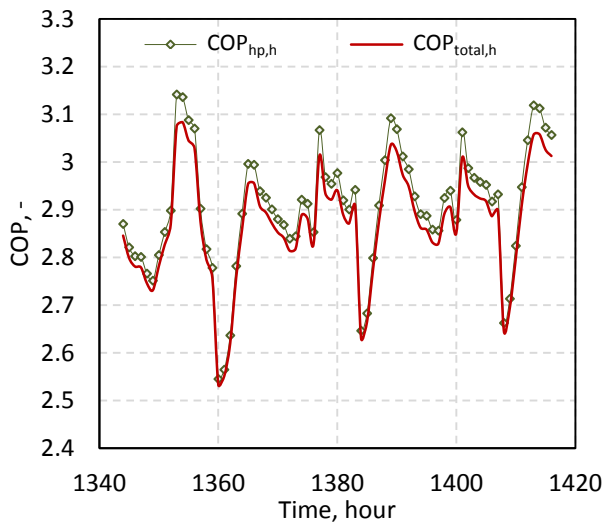


Fig. 16 - COP_h value under different indoor heating loads

Fig. 17 - Heat transfer amounts of different CO_2 heat pump components for the indoor heating mode

The heat transfer rate and power consumption of the different components for the indoor heating mode are shown in Figure 17. Similarly, the \dot{Q}_h refers to the heating capacity of the heat pumping system. The power consumption of the compressor is mainly dependant on the heating load of the system. Figures 18 and 19 show the gas cooling and evaporating pressures and the working fluid temperature variation under different indoor heating loads. The supply water temperature is 45 °C, and the variation of the building load accounts for the variation of the pressure and temperature in the different components.

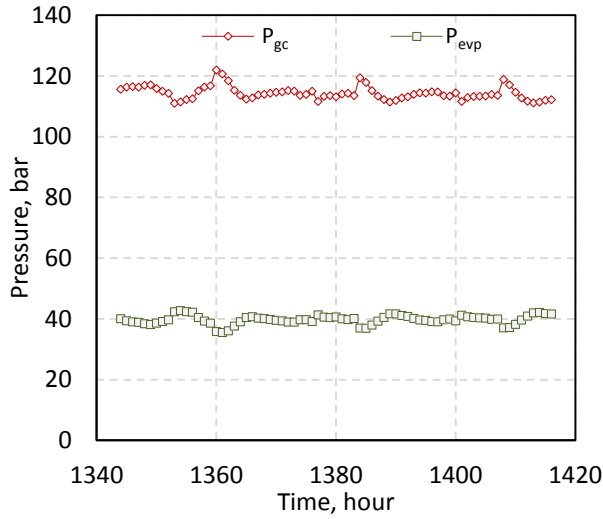


Fig. 18 - Gas cooling and evaporating pressure under different indoor heating loads

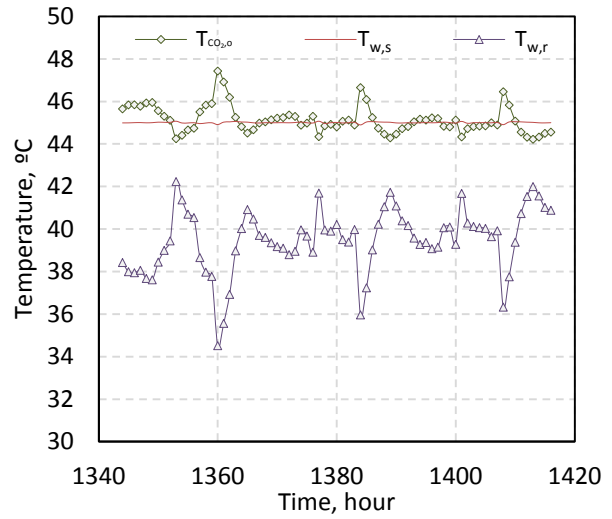


Fig. 19 - Working fluid temperature variation under different indoor heating loads

Figure 20 showed the simulation results of the COP_h variation under different indoor heating loads for various Φ_{air} values. It can be observed that the lower Φ_{air} value gives the higher COP_h , but the difference is not as obvious as for that of the indoor cooling mode. This is mainly because there is no airside fan power consumption for the indoor heating mode, and the power consumption for a hydraulic pump is very small compared with that of a compressor.

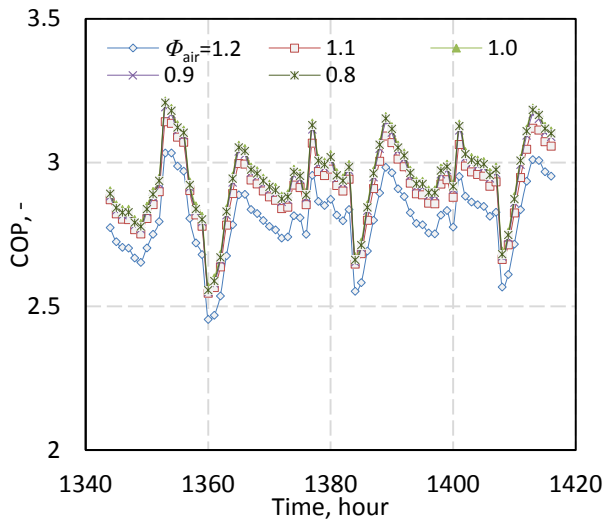


Fig. 20 - COP_h value variation under different Φ_{air} values with different indoor heating loads

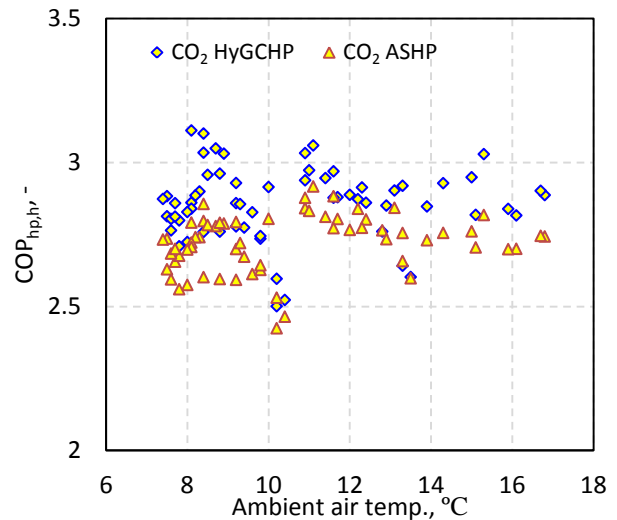


Fig. 21 - COP_h comparison for the CO_2 HyGCHP and ASHP at different ambient air temperatures

At last, the heating performance of the CO_2 hybrid GCHP and the ASHP system at different ambient air temperatures is also compared for the investigated heating periods. Figure 21 shows the simulated COP_h results of these two systems under the ambient air temperature range of 7.5~17 °C. It can be observed that the cooling performance of the CO_2 hybrid GCHP system is slightly better than that of the ASHP system,

and the calculated averaged COP_h values are 2.86 and 2.73. This shows that the averaged performance improvement is 4.7 %. This improvement also benefits from the higher and constant borehole temperature, which can increase the evaporating temperature or pressure to reduce the compressing work.

5. Conclusion

In this work, the steady state and quasi-steady state analysis on a CO₂ hybrid ground-coupled heat pumping system is performed for the warm climate. The main objectives are to determine the optimal control strategy of the gas cooler pressure and to predict the practical energy efficiency of the CO₂ hybrid ground-coupled heat pumping system.

1. The steady state analysis well supported the fundamental design procedure for the quasi-steady state and practical model of the system, and the optimal control strategy of the gas cooler pressure was proposed for the CO₂ hybrid transcritical cycle.
2. The quasi-steady state analysis of the CO₂ hybrid ground-coupled heat pumping system predicted a practical energy efficiency of the system. The time-dependent COP values under different indoor heating or cooling loads are shown. The $COP_{total,c}$ varies from 2.2 to 4.1, while the $COP_{total,h}$ varies from 2.53 to 3.15, according to the hourly simulation results.
3. The system performance with different Φ_{air} values is also discussed, and it proves that a lower Φ_{air} value gives the higher system performance due to the lower operating gas cooling pressure, which is determined by the optimal control strategy.
4. And last, the heating and cooling performance of the CO₂ hybrid GCHP and ASHP system at different ambient air temperatures is compared, and the averaged COP improvements are 28.1% and 4.7%, respectively, for the typical heating and cooling days' operation.

Reference

- ANSI/AHRI Standard. 2011. Standard for performance rating of water-chilling and heat pump water-heating packages using the vapour compression cycle. ANSI/AHRI Standard 550/590 (I-P)
- Byrne, P., Miriel, J., Lenat, Y., 2009, Design and simulation of a heat pump for simultaneous heating and cooling using HFC or CO₂ as a working fluid, *Int. J. Refrig.*, 32, 1711–1723
- Deng, S., Dai, Y.J., Wang, R.Z., 2013, Performance optimization and analysis of solar combi-system with carbon dioxide heat pump, *Sol. Energ.*, 98, 212–225
- Esen H., Inalli M., Esen M., 2007. A techno-economic comparison of ground-coupled and air-coupled heat pump system for indoor cooling. *Build. Environ.*, 42(5):1955–1965.
- Esen H., Esen M., Ozsolak O., 2015. Modelling and experimental performance analysis of solar-assisted ground source heat pump system. *J. Exp. Theor. Artif. Intell.*, pp. 1–17 , <http://dx.doi.org/1080/0952813X.2015.1056242>

- 1
2
3
4
5
6
7
8
9
10
11
12
13
14
15
16
17
18
19
20
21
22
23
24
25
26
27
28
29
30
31
32
33
34
35
36
37
38
39
40
41
42
43
44
45
46
47
48
49
50
51
52
53
54
55
56
57
58
59
60
61
62
63
64
65
- Goel, S., Rosenberg, M., Athalye, R., Xie, Y., Wang, W., Hart.,R. Zhang, J., Mendon, V., 2014. Enhancements to ASHRAE Standard 90.1 Prototype Building Models, Pacific Northwest National Laboratory, PNNL-23269
- Haaf, S., 1988, Wärmeübertragung in Luftkühlern, Handbuch der Kältechnik, Bd. 6, Teil B: Wärmeaustauscher, Berlin u.a.: Springer Verlag, 435–491
- Hafner, A., Claussen, I.C., Schmidt, F., Olsson, R., Fredslund, K., Eriksen, P.A., Madsen, K.B., 2014, Efficient and integrated energy systems for supermarkets. 11th IIR Gustav Lorentzen Conference on Natural Working Fluids. Hangzhou, China, IIF/IIR: P69
- Hafner, A., Alonso, M. J., Schmäzle, C., Neksa, P., 2013. High efficient 18-90 m³/h R744 compressor. 8th International Conference on Compressors and Coolants, Proceedings: 166-174
- Jakobsen, A., Skaugen, G., Skiple, T., Neksa, P., Andresen, T., 2004. Development and evaluation of a reversible CO₂ residential air conditioning system compared to a state of the art R-410A unit. 6th IIR Gustav Lorentzen Conference on Natural Working Fluids. Glasgow, IIF/IIR: P66.
- Jakobsen, A., Skiple, T., Neksa, P., Wachenfeldt, B., Skaugen, G., 2007. Development of a reversible CO₂ residential air conditioning system. 22nd Int. Congress of Refrigeration, Beijing, IIF/IIR: 2170-2179.
- Kavanaugh, S. P., 1998. A design method for hybrid ground-source heat pumps. ASHRAE Trans. 104(2):691–8.
- Liao, S.M., Zhao, T.S., Jakobsen, A., 2000. Correlation of optimal heat rejection pressures in transcritical carbon dioxide cycles. Appl. Therm. Eng., 20 (9), 831-841.
- Lorentzen, G., 1990. Trans-critical vapour compression cycle device. Patent WO/07683.
- Man, Y., Yang, H.X., Wang, J.G., 2010. Study on hybrid ground-coupled heat pump system for air-conditioning in hot-weather areas like Hong Kong. Appl. Energ., 87 (9): 2826-2833.
- Masson, N., 2015. GUIDE to Natural Refrigerants, state of the industry North America & in the world, 4th annual ATMOSphere America 2015, Atlanta, Presentation.
- Neksa, P., Walnum, H.T., Hafner, A., 2010. CO₂ - A refrigerant from the past with prospects of being one of the main refrigerants in the future. 9th IIR Gustav Lorentzen Conference on Natural Working Fluids, Sydney, IIF/IIR: P21.
- Park., C.Y., Hrnjak P.S., 2007, CO₂ and R410A flow boiling heat transfer, pressure drop, and flow pattern at low temperatures in a horizontal smooth tube, Int. J. Refrig., 30: 166–178.
- Richter, C., 2008, Proposal of new object-oriented equation-based model libraries for thermodynamic systems. Dissertation, Technische Universität Braunschweig.
- Thome., J.R., Ribatski., G., 2005, State-of-the-art of two-phase flow and flow boiling heat transfer and pressure drop of CO₂ in macro- and micro-channel, Int. J. Refrig., 28: 1149–1168.
- Wetter, M., Zuo, W., Nouidui, T., Pang, X., 2013. Modelica buildings library. Journal of Building Performance Simulation, 7(4):253–70.
- Yu, X., Wang, R.Z., Zhai, X.Q., 2011, Year round experimental study on a constant temperature and humidity air-conditioning system driven by ground source heat pump, Energy 36, 1309–1318